ORIGINAL ARTICLE

Comparison of the Bone Forming Ability of Different Sized-alpha Tricalcium Phosphate Granules using a Critical Size Defect Model of the Mouse Calvaria

**Tomoko TOKUDA[1], Yoshitomo HONDA[2],
Yoshiya HASHIMOTO[3], and Naoyuki MATSUMOTO[4]**

*[1]Graduate School of Dentistry (Department of Orthodontics),
[2] Institute of Dental Research, [3] Department of Biomaterials,
[4] Department of Orthodontics, Osaka Dental University, Osaka, Japan*

Synopsis

Alpha-tricalcium phosphate (α-TCP) has been investigated extensively as an artificial bone graft; however, the relationship between size of α-TCP particles and its bone-formation capability is not clear. In the present study, we compared the bone-formation capability of two different sized porous α-TCP particles (α-TCP200 [under 200 μm], and α-TCP600 [500–600 μm]) in critical-sized bone defects in mouse calvaria up to 12 wk after implantation. Scanning electron microscopy revealed that both particles possessed similar smooth surface with porous structure. Before implantation, inter-particle size and specific surface area of α-TCP200 were 27 μm and 0.40 m^2/g and of α-TCP600 were 209 μm and 0.24 m^2/g, respectively. Histomorphometric analysis after implantation of the particles revealed that both particles promoted osteoconduction. At 12 wk, α-TCP200 induced superior bone formation than α-TCP600. At 4 wk, α-TCP200 showed more hydrolysis than α-TCP600. These results indicate that the size of α-TCP particles may influence their bone-formation capability in critical-sized bone defects of mouse calvaria. This effect might be partially due to the difference in the hydrolysis speed of different-sized particles.

Key words: *alpha tricalcium phosphate, bone formation, particle, calvaria, hydrolysis*

Introduction

Bone defects attributed to serious periodontitis, trauma, and injury are commonly encountered in the fields of dentistry, craniofacial surgery, and orthopedics. Although autogenous bone grafting is still considered the gold standard for treatment, this process has several drawbacks, such as the requirement of a second surgery and the limited availability of collectable bone [1]. Artificial bone grafts are thought to be promising alternatives to autogenous bone grafts. Several calcium phosphate (CaP)-based biomaterials, such as hydroxyapatite (HA), tricalcium phosphate (TCP), and octacalcium phosphate (OCP), have been intensively investigated for use as artificial bone because, under appropriate conditions, these materials show excellent biocompatibility and bioactivity [2, 3].

High-temperature TCP, known as alpha-tricalcium phosphate (α-TCP), is often prepared by the sintering of amorphous precursors with the proper composition [4]. Its calcium-to-phosphate ratio is theoretically 1.50. In general, α-TCP dissolves more easily than OCP, β-TCP, and HA under neutral pH conditions [4]. Furthermore, α-TCP converts to apatite in aqueous solution over time [5], to low-

crystalline hydroxyapatite in simulated body fluid [6], to fluoride-incorporated apatite in sodium fluoride solution [7], and to OCP in phosphoric acid solution [8].

Numerous studies have been performed to verify the usability of α-TCP for clinical application as bone graft material [9, 10]. α-TCP has been found to be biodegradable in rabbit cranial defects when used in the particle form [9] and in Ti-chambers when used in the porous block form [10]. This ceramic is known to be a component of self-setting calcium phosphate cements, which can be injected into bone defects [11]. α-TCP is often used as a carrier for drugs, such as statin [12], catechin [13], and growth factors [14]. It provides a good environment for osteogenesis of MSCs [15] and osteoblastic cells [16] even *in vitro*.

In previous studies using different CaPs, it has been recognized that its bone-formation capability is affected by some properties such as bioresobabiliy, pore size, and mechanical strength [17]. Particle size has also been reported as a pivotal property influencing the result of bone formation [18-22]. Consistent with these studies, we have recently reported that different-sized α-TCP particles with artificial polypeptides induced distinct bone formation in a mini-pig non-critical-sized skull defect model [1]. This finding suggested that particle size might be a factor modulating the bone formation capability of α-TCP. However, our previous study was performed under the conditions with artificial polypeptides. There is still paucity of information about the relationship between particle size of intact α-TCP particles (those not exposed to treatments such as hydrolysis and not mixed with materials such as polymers) and its bone-formation capability in bone defects.

To elucidate this relationship, we investigated whether size of α-TCP particles without any intrusion, such as polypeptide, alter its bone-formation capability in critical-sized defect of mouse calvaria. Two different-sized α-TCPs were prepared with particle size <200 μm and 500–600 μm (hereafter, referred to as α-TCP200 and α-TCP600, respectively). In addition, we also evaluated the hydrolysis behavior of the two α-TCPs at 4 wk after implantation.

Materials and methods

1. Preparation and characterization of α-TCP particles

Two types of porous α-TCPs with different particle sizes were kindly provided by Taihei Chemical Industrial Co. Ltd. (Osaka, Japan). The particle sizes of the two α-TCPs were similar to those used in the previous study in order to compare the results easily [1]. A field emission-scanning electron microscope (FE-SEM; S-4100, Hitachi High-Technologies Corporation, Tokyo, Japan) was used to analyze particle size, pore distribution, and outer surface conditions. Before observation, samples were coated with the platinum-palladium using E-1030 (Hitachi High-Technologies Corporation). α-TCP particles were characterized by the powder X-ray diffraction system (XRD; XRD-6100, Shimadzu, Kyoto, Japan). XRD patterns were obtained under the following condition: 40.0 kV, 30.0 mA, scan rate 2 degree/min with a step size 0.05 degrees, 3–80 degrees. Crystal phase was characterized with database from the International Centre for Diffraction Data (HA: 9-0432; α-TCP: 9-0348). Specific surface area (SSA) of the α-TCPs was evaluated by the Bet method using Gemini 2360 (Shimadzu). Inter-particle size of α-TCP particles before implantation was determined by the mercury intrusion technique using auto pore IV 9510 (Micromeritics, Norcross, GA, USA).

2. Implantation of α-TCPs into critical-sized bone defect of mouse calvaria

All *in vivo* experiments were conducted in accordance with the guidelines of the local animal ethics committee of Osaka Dental University and were approved by the committee (approval number: 12-05001). Male ICR mice (8 wk) were housed in a light and temperature controlled environment during the experiment. Following general anesthesia with intraperitoneal injection of sodium pentobarbital supplemented with isoflurane inhalation, the skin and periosteum was opened under the disinfection conditions. Next, 4.2 mm defects, which have been reported as critical-sized defects [23], were created at the calvaria by using the trephine bar (Dentech, Tokyo, Japan) under saline irrigation so as not to damage the one. After the defects were filled

with samples or left unfilled (control), they were covered with 50-μm Teflon sheet to stabilize the implants. At least 4 mice were used for each group. Four or 12 wk after the treatment, the calvaria of each mouse was obtained to for use in further experiments. The calvaria was partially fixed with cold 4% paraformaldehyde phosphate buffer solution before microfocus X-ray computed tomography (μCT) and histological analysis. Calvariae without fixation were used for estimating the hydrolysis behavior of particles *in vivo*.

3. Micro-computed tomography

After fixation, the specimens were evaluated using μCT (SMX-130CT, Shimadzu). Calvariae were placed on the turntable using utility wax, and then exposed to 74 μA of 48 kV radiation at 46.8 μm intervals. Images were saved at 512 × 512 pixel. The μCT images from vertical and lateral sides were reconstructed using the TRI/3D bone software (Ratoc Co. Ltd., Tokyo Japan). Bone mineral density (BMD) representing calcified bone tissue was evaluated using cylindrical phantoms containing a hydroxyapatite (HA content: 200 to 800 mg/cm^3).

4. Histology and histomorphometric analysis

After fixation, the samples were decalcified, dehydrated, and embedded in paraffin. The specimens were sectioned at 5 μm thickness and used for hematoxylin-eosin staining (H-E staining). Histomorphometric analysis of bone formation in the defects was conducted according to the method reported previously [3]. In brief, H-E-stained sections covering the whole defect were used to calculate the extent of new bone formation. The area of tissue showing color

similar to that of the non-treated calvaria was estimated as the area of newly formed bone (NB area), while the whole area created by the trephination was considered the treated area (TA). Both NB and TA were analyzed using Image J software (version 1.46r, NIH, USA). The percentage of newly formed bone was calculated as (NB/TA) × 100.

5. Hydrolysis of α-TCP particles in the bone defect

At 4 wk after implantation, the particles, along with the tissue, were isolated without fixation. The complexes were grained with mortar and pestle, and then evaluated by XRD analysis to estimate the hydrolysis behavior. The particles in the defects of three mice were integrated in order to analyze the hydrolysis rate of α-TCPs.

6. Statistical analysis

All data in bar graph were expressed as the mean with standard deviation. One-way analysis of variance (ANOVA) was used to compare the difference of the means among groups. Tukey-Kramer test was used as a post hoc test to confirm difference noted in ANOVA.

Results
1. Characterization of α-TCP particles

Fig. 1A shows the macroscopic structure of α-TCP200 and α-TCP600. We confirmed that fine (α-TCP200) and coarse (α-TCP600) particles were obtained. Consistent with this difference, α-TCP200 showed larger SSA than α-TCP600: 0.40 m^2/g for α-TCP200 and 0.24 m^2/g for α-TCP600. Fig. 1B shows the electron microscopic images of α-TCPs. Except for the difference in particle size, there was negligible

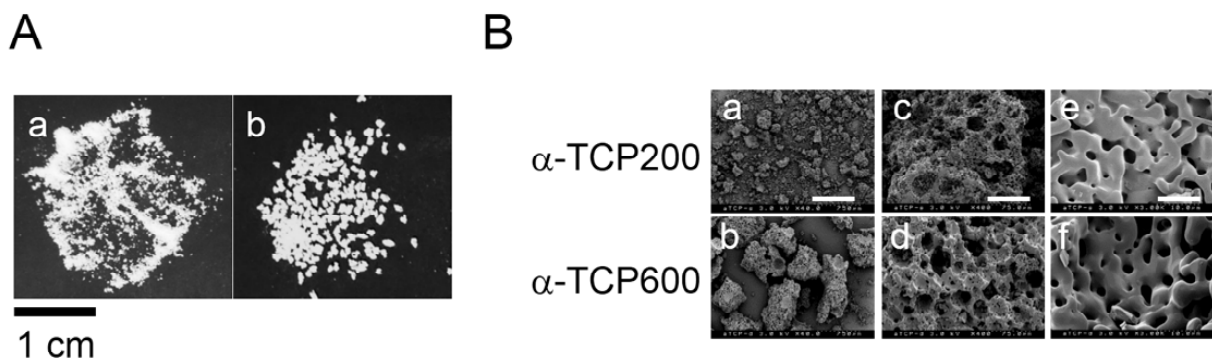**Fig. 1**   Macroscopic (A) and scanning electron microscopic (B) images of α-TCPs.
A-a: α-TCP200; A-b: α-TCP600. Bars in B: 750 μm for a, b; 75 μm for c, d; 10 μm for e, f.

difference in the surface structure of the two particles. At high magnification, both α-TCPs showed macropores of varying sizes and smooth surfaces. XRD profiles of both intact particles are shown in Fig. 2A. The specific peaks of α-TCP (indicated by the triangles) were detectable in the XRD patterns of both particles. Inter-particle size (median diameter) of α-TCP200 was estimated as 27 μm, while that of α-TCP600 was 209 μm (Fig. 3).

2. Control group

Fig. 4A and B show the μCT (vertical and lateral angle) and BMD (vertical) images of the defect in the control group. There was no enhancement in the radiopacity of the defect up to 12 wk after implantation. Fig. 4C and D display the histological sections of defect at 12 wk. Thin connective tissue entirely covered the defect from edge to edge (Fig. 4D-b).
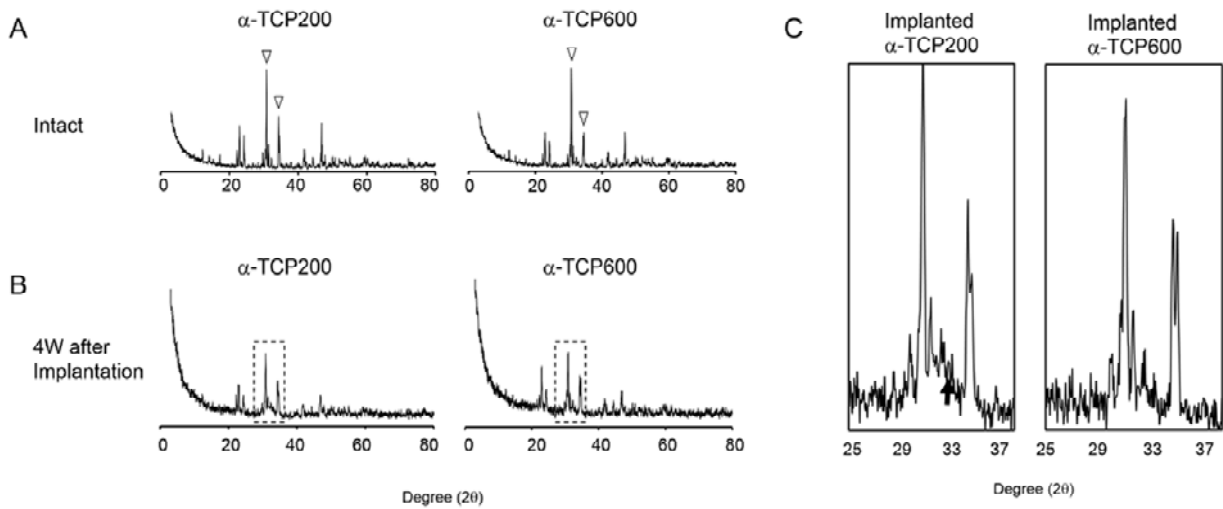

Fig. 2 X-ray diffraction pattern of samples before (A) and after (B, C) the implantation. Intact: without hydrolysis treatment (original particle). Triangles: specific peaks of α-TCP. Broken squares in B show the magnified area used in C. Arrow in C: specific peak of apatite at 32.9°.
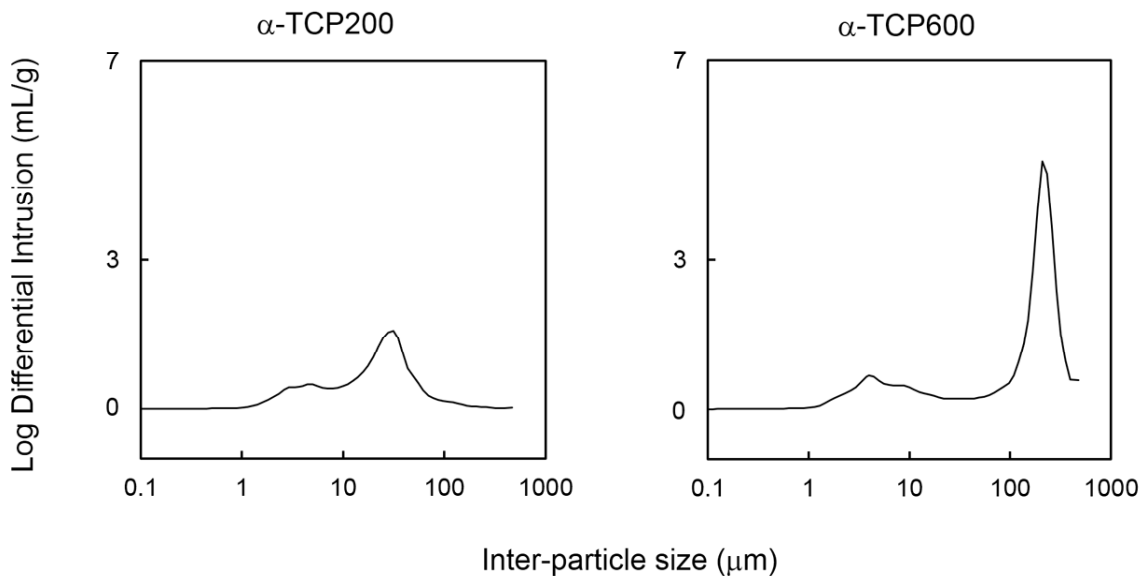

Fig. 3 Inter-particle size of α-TCPs analyzed by the mercury intrusion technique.
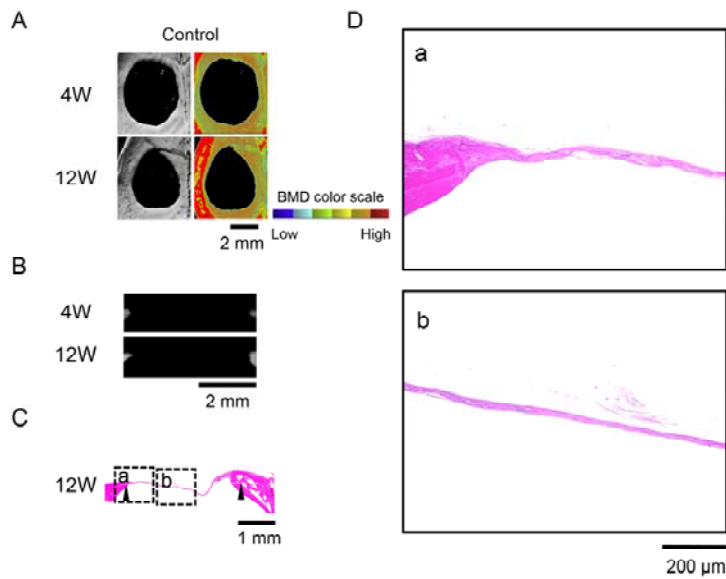
Fig. 4 Bone formation in defect treated without α-TCPs (control group).
A: vertical micro-computed tomography (μCT) and bone-mineral density (BMD) images. B: lateral μCT image. C, D: histological sections of defect stained with hematoxylin-eosin (H-E). Gap of triangles: created bone defect. Broken squares in C: magnified area for D.
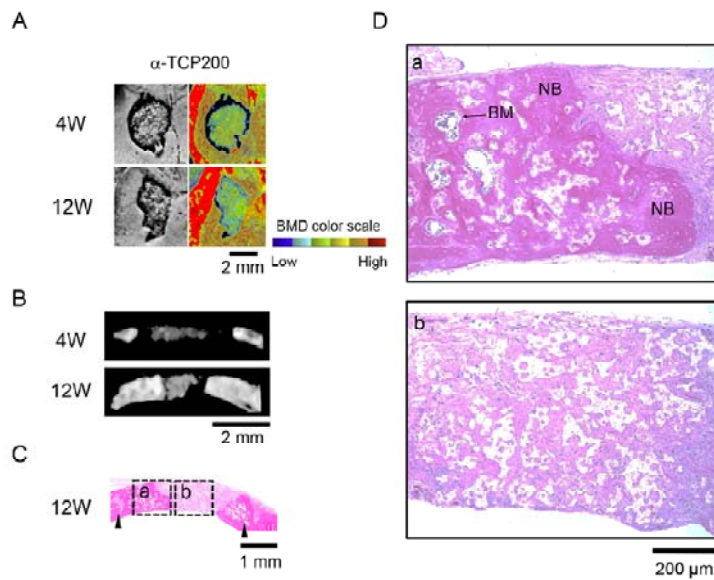

Fig. 5 Bone formation in defects treated with α-TCP200.
A: vertical μCT and BMD images. B: lateral μCT images. C, D: histological sections of defect stained with H-E. Broken squares in C: magnified area for D. Gap of triangles: created bone defect. NBs: New bones. BM: Bone marrow.
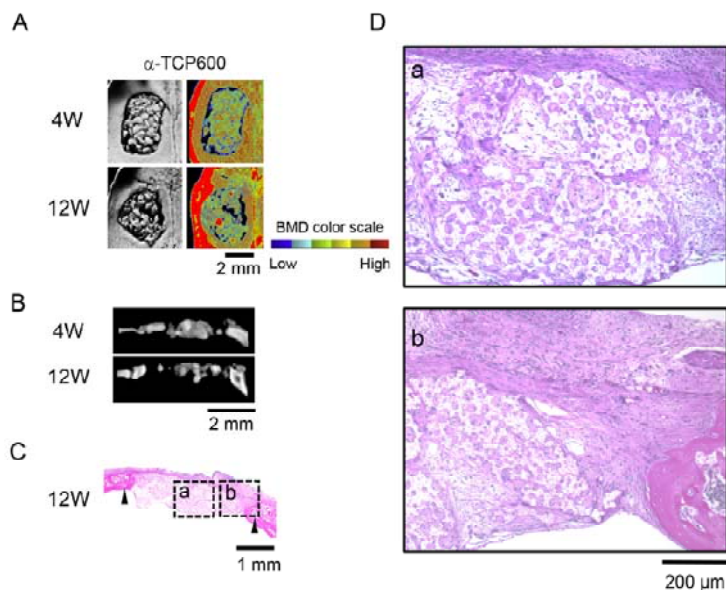

Fig. 6 Bone formation in defect treated with α-TCP600.
A: vertical μCT and BMD images. B: lateral μCT images. C, D: histological sections of defect stained with H-E. Gap of triangles: created bone defect. Broken squares in C: magnified area for D.

3. α-TCP200

Fig. 5A and B show the μCT (vertical and lateral angle) and BMD (vertical) images of defects treated with α-TCP200. Strong radiopacity gradually covered the defects. Higher BMD, shown in brown, invaded from the edge of defects. Fig. 5C and D shows the histological section of the defect treated with α-TCP200. Consistent with the result in the BMD image, new bone formation increased and proceeded toward the center of the defects. At high magnification, the newly formed bone was observed to cover the blank white portion, possibly indicating residual α-TCP particles in the defect. We could observe bone marrow containing blood cells in the newly formed bone. In addition, fibrous tissue could still be observed in the center of the defects.

4. α-TCP600

Fig. 6A and B show the μCT (vertical and lateral angle) and BMD (vertical) images of defects treated with α-TCP600. Although radiopacity could be observed in the defects up to 12 wk, its integration was subtle compared with that in the α-TCP200 samples. Fig. 6C and D show the histological section of defects treated with α-TCP600. The blank white portion covered by cells possibly indicates residual α-TCP600 particles in the defect. Large α-TCP600 particles were still visible (Fig. 6D-a). Despite cell invasion, there was no remarkable ingrowth of bone toward the center of the defect. New bone formation was limited to the edge of the defect (Fig. 6D-b).

5. Histomorphometric analysis of bone formation

Histomorphometric analysis of bone formation in the defect revealed that both α-TCPs induced greater bone formation than that in control group within 4 wk, with negligible difference between the two α-TCPs (Fig. 7). At 12 wk after implantation, new bone formation in the α-TCP200 samples was significantly greater than that in the α-TCP600 samples.
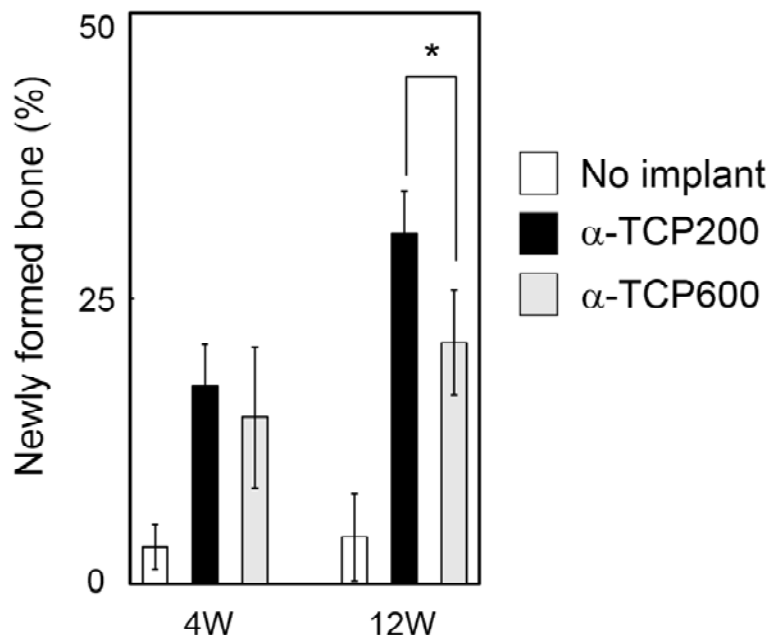

Fig. 7 Histomorphometric analysis of new bone formation induced by α-TCP implantation. Data show the mean with standard deviation (N=4). *$P < 0.05$: Significant difference between α-TCP200 and α-TCP600 at 12 wk (ANOVA with Tukey-Kramer test).

6. Hydrolysis of α-TCP particles in vivo

Fig. 2B and C show the XRD patterns of the implanted α-TCPs particles at 4 wk after implantation. A gentle bulge could be observed around 30–33° for α-TCP200, which is similar to the pattern reported for apatite [6] (Fig. 2B and C). The specific peak of apatite could be observed at 32.9° in the pattern of implanted α-TCP200. There was a subtle change in the pattern for implanted α-TCP600, suggesting that α-TCP200 converted faster than α-TCP600.

Discussion

α-TCP is widely considered as a candidate for use as bone grafting material. However, few studies have investigated the relationship between α-TCP particle size and its bone-formation ability. In the present study, we present evidence that α-TCP200 induced superior bone formation compared with α-TCP600 in the critical-sized defect of mouse calvaria. The difference was more obvious at 12 wk after implantation. We did not observe any inflammation at 4 and 12 wk, suggesting that both α-TCPs must be adequately biocompatible as bone graft scaffolds.

Although the effect of inter-particle size, corresponding with pore size, on bone formation is still controversial, values above 100 μm have been proposed as a preferable condition for bone formation using CaP [20]. Consistent with this report, Galois *et al*. have reported that HA with 45–80 μm pore size induced inferior bone formation speed compared with HA with larger pore sizes (80–140, 140–200, and 200–250 μm) in femoral condyles of rabbits [24]. Furthermore, our pervious study using OCP particles showed that large particles (500–1000 μm), with inter-particle size 176.6 μm, induced greater bone formation than did small particles (53–300 μm), with inter-particle size 28.8 μm [18]. In the present study, inter-particle size of α-TCP200 (27 μm) was smaller than that of α-TCP600 (209 μm) before implantation (Fig. 3). The bone-formation capability of α-TCP was hardly affected by its small inter-particle size. There was enough cell invasion in the α-TCP200-implanted site at 12 wk (Fig. 5). This discrepancy might be due to the high biodegradability

of α-TCP. Kihara *et al* reported that α-TCP gradually degrades in the bone defect [9], suggesting that the inter-particle size of α-TCP was likely to increase with time after implantation. These results indicate that, at the time of surgery, inter-particle size over 100 μm is not always necessary for induction of bone regeneration by α-TCP particles.

In the previous study, we have reported that the particle size of α-TCP in the artificial collagen sponge modified the bone-formation capability of the scaffold in skull defect in mini-pigs. Three different-sized particles were used for the experiment (small, 136.2 μm; large, 580.8 μm; large and small mixed, 499.3 μm) [1]. The mixed particles yielded superior bone formation than the other two. Given the amount of artificial collagen was same in all three scaffolds, pore size distribution would be approximately similar among the samples, suggesting that other properties of α-TCP might influence its bone formation ability. In this study, α-TCP200, the smaller particle, showed better bone-formation ability than the large particle (α-TCP600) (Fig. 7). Although we could not elucidate the complete mechanism, hydrolysis behavior of α-TCPs might be partially involved in the process. As shown in Fig. 2, α-TCP200 transformed to apatite faster than α-TCP600 even *in vivo*. Hydrolysis of α-TCP is known to alter the concentration of calcium and phosphate ions around the crystals [6]. The ions can modulate osteoblast differentiation and proliferation of stem cells [25, 26]. Furthermore, Liu *et al* reported that adequate amount of α-TCP induced osteoblastogenesis [15]. The faster hydrolysis of α-TCP200 might provide an appropriate environment for the cells to differentiate into bone cells or to form new bone.

In the present study, we could not observe well-crystallized apatite XRD pattern at 10.8° even in the α-TCP200 samples, although there were differences around 32° after transplantation *in vivo*. The hydrolysis velocity of α-TCP200 seems to be slower than that reported by other studies performed *in vitro* [6] (Fig. 2). This attenuation of hydrolysis might be due to the adsorption of the protein in the body fluid. A previous study showed that FBS effectively delayed

the hydrolysis of α-TCP in the culture medium [27]. The various proteins in serum are known to modulate nucleation of calcium phosphate [28]. It is suggested that the serum contained various growth factors or other factors capable of controlling cell fate [29]. Different crystal phase induces distinct protein adsorption on products [30]. In the present study, hydrolysis of α-TCP200 likely changed its surface character, causing different proteins to be attracted. These adsorbed proteins could have contributed to the enhanced bone-formation capability of α-TCP200.

The present study showed that the bone-formation capability of α-TCP200 is superior to that of α-TCP600 in critical-sized defect of mouse calvaria. However, the experiment was performed under conditions of limitations. The α-TCP particles used possessed macropores at the surface. Surface characters of materials are known to affect the results of bone formation. Different-sized particles might be necessary for obtaining optimal bone regeneration at different transplantation sites. It is still unclear how the cells responded to the hydrolysis of α-TCPs *in vitro*. Our results provide insights into the usability of α-TCP particles in bone regeneration therapy. However, in view of the above-mentioned issues, further detailed examination would be essential to determine the optimal size of α-TCP particles for application in clinical practice.

Conclusion
In the present study, two α-TCPs with different particle sizes induced distinct bone formation in critical-sized bone defect of mouse calvaria. These two α-TCPs showed different hydrolysis behaviors at 4 wk after implantation. These results indicate that the particle size of α-TCPs may affect their bone-formation capability. The influence of particle size could partially be due to the difference in the hydrolysis rate of the different-sized α-TCP particles.

References
1) Sakai K, Hashimoto Y, Baba S, Nishiura A, Matsumoto N. Effects on bone regeneration when collagen model polypeptides are combined with various sizes of alpha-tricalcium phosphate particles. Dent Mater J 2011; 30: 913-922.
2) Pryor LS, Gage E, Langevin CJ, Herrera F, Breithaupt AD, Gordon CR, Afifi AM, Zins JE, Meltzer H, Gosman A, Cohen SR, Holmes R. Review of bone substitutes. Craniomaxillofac Trauma Reconstr 2009; 2: 151-160.
3) Honda Y, Anada T, Kamakura S, Morimoto S, Kuriyagawa T, Suzuki O. The effect of microstructure of octacalcium phosphate on the bone regenerative property. Tissue Eng Part A 2009; 15: 1965-1973.
4) Carrodeguas RG, De Aza S. Alpha-Tricalcium phosphate: synthesis, properties and biomedical applications. Acta Biomater 2011; 7: 3536-3546.
5) Yubao L, Xingdong Z, de Groot K. Hydrolysis and phase transition of alpha-tricalcium phosphate. Biomaterials 1997; 18: 737-741.
6) Uchino T, Yamaguchi K, Suzuki I, Kamitakahara M, Otsuka M, Ohtsuki C. Hydroxyapatite formation on porous ceramics of alpha-tricalcium phosphate in a simulated body fluid. J Mater Sci Mater Med 2010; 21: 1921-1926.
7) TenHuisen KS, Brown PW. Hydrolysis of alpha-tricalcium phosphate in NaF solutions. Biomaterials 1999; 20: 427-434.
8) Bigi A, Boanini E, Botter R, Panzavolta S, Rubini K. Alpha-tricalcium phosphate hydrolysis to octacalcium phosphate: effect of sodium polyacrylate. Biomaterials 2002; 23: 1849-1854.
9) Kihara H, Shiota M, Yamashita Y, Kasugai S. Biodegradation process of alpha-TCP particles and new bone formation in a rabbit cranial defect model. J Biomed Mater Res B Appl Biomater 2006; 79: 284-291.
10) Yamada M, Shiota M, Yamashita Y, Kasugai S. Histological and histomorphometrical comparative study of the degradation and osteoconductive characteristics of alpha- and beta-tricalcium phosphate in block grafts. J Biomed Mater Res B Appl Biomater 2007; 82: 139-148.
11) Oh SA, Lee GS, Park JH, Kim HW. Osteoclastic cell behaviors affected by the alpha-tricalcium phosphate based bone cements. J Mater Sci Mater Med 2010; 21: 3019-3027.
12) Varalakshmi PR, Kavitha M, Govindan R, Narasimhan S. Effect of statins with

α-tricalcium phosphate on proliferation, differentiation, and mineralization of human dental pulp cells. J Endod 2013; 39: 806-812.

13) Rodriguez R, Kondo H, Nyan M, Hao J, Miyahara T, Ohya K, Kasugai S. Implantation of green tea catechin alpha-tricalcium phosphate combination enhances bone repair in rat skull defects. J Biomed Mater Res B Appl Biomater 2011; 98: 263-271.

14) Honnami M, Choi S, Liu Il, Kamimura W, Taguchi T, Hojo H, Shimohata N, Ohba S, Koyama H, Nishimura R, Chung U-i, Sasaki N, Mochizuki M. Bone regeneration by the combined use of tetrapod-shaped calcium phosphate granules with basic fibroblast growth factor-binding ion complex gel in canine segmental radial defects. J Vet Med Sci 2014; 76: 955-961.

15) Liu J, Zhao L, Ni L, Qiao C, Li D, Sun H, Zhang Z. The effect of synthetic α-tricalcium phosphate on osteogenic differentiation of rat bone mesenchymal stem cells. Am J Transl Res 2015; 7: 1588-1601.

16) Ehara A, Ogata K, Imazato S, Ebisu S, Nakano T, Umakoshi Y. Effects of alpha-TCP and TetCP on MC3T3-E1 proliferation, differentiation and mineralization. Biomaterials 2003; 24: 831-836.

17) Hannink G, Arts JJ. Bioresorbability, porosity and mechanical strength of bone substitutes: what is optimal for bone regeneration? Injury 2011; 42 Suppl 2: S22-25.

18) Murakami Y, Honda Y, Anada T, Shimauchi H, Suzuki O. Comparative study on bone regeneration by synthetic octacalcium phosphate with various granule sizes. Acta Biomater 2010; 6: 1542-1548.

19) Tanuma Y, Anada T, Honda Y, Kawai T, Kamakura S, Echigo S, Suzuki O. Granule size-dependent bone regenerative capacity of octacalcium phosphate in collagen matrix. Tissue Eng Part A 2012; 18: 546-557.

20) Coathup MJ, Cai Q, Campion C, Buckland T, Blunn GW. The effect of particle size on the osteointegration of injectable silicate-substituted calcium phosphate bone substitute materials. J Biomed Mater Res B Appl Biomater 2013; 101: 902-910.

21) Murai M, Sato S, Fukase Y, Yamada Y, Komiyama K, Ito K. Effects of different sizes of beta-tricalcium phosphate particles on bone augmentation within a titanium cap in rabbit calvarium. Dent Mater J 2006; 25: 87-96.

22) Felipe M, Andrade P, Novaes AJ, Grisi M, Souza S, Taba MJ, Palioto D. Potential of bioactive glass particles of different size ranges to affect bone formation in interproximal periodontal defects in dogs. J Periodontol 2009; 80: 808-815.

23) Aalami OO, Nacamuli RP, Lenton KA, Cowan CM, Fang TD, Fong KD, Shi Y-Y, Song HM, Sahar DE, Longaker MT. Applications of a mouse model of calvarial healing: Differences in regenerative abilities of juveniles and adults. Plastic Reconstr Surg 2004; 114: 713-720.

24) Galois L, Malinard D. Bone ingrowth into two porous ceramics with different pore sizes : An experimental study. Acta Orthop Belg 2004; 70: 598-603.

25) Dvorak MM, Siddiqua A, Ward DT, Carter DH, Dallas SL, Nemeth EF, Riccardi D. Physiological changes in extracellular calcium concentration directly control osteoblast function in the absence of calciotropic hormones. Proc Natl Acad Sci U S A 2004; 101: 5140-5145.

26) Beck GJ, Moran E, Knecht N. Inorganic phosphate regulates multiple genes during osteoblast differentiation, including Nrf2. Exp Cell Res 2003; 288: 288-300.

27) Lee JT, Leng Y, Chow KL, Ren F, Ge X, Wang K, Lu X. Cell culture medium as an alternative to conventional simulated body fluid. Acta Biomater 2011; 7: 2615-2622.

28) Tagaya M, Ikoma T, Takeguchi M, Hanagata N, Tanaka J. Interfacial serum protein effect on biological apatite growth. J Phys Chem C 2011; 115: 22523-22533.

29) Honda Y, Ding X, Mussano F, Wiberg A, Ho CM, Nishimura I. Guiding the osteogenic fate of mouse and human mesenchymal stem cells through feedback system control. Sci Rep 2013; 3: 3420.

30) Kaneko H, Kamiie J, Kawakami H, Anada T, Honda Y, Shiraishi N, Kamakura S, Terasaki T, Shimauchi H, Suzuki O. Proteome analysis of rat serum proteins adsorbed onto synthetic octacalcium phosphate crystals. Anal Biochem 2011; 418: 276-285.

Corresponding author:
Yoshitomo HONDA, DDS, Ph.D
8-1, Kuzuhahanazonocho, Hirakata, Osaka, 573-1121, Japan
Institute of Dental Research,
Osaka Dental University
TEL: +81-72-864-3130
FAX: +81-72-864-3150
E-mail: honda-y@cc.osaka-dent.ac.jp